Structure and X-ray reference diffraction patterns of $(Ba_{6-x}Sr_x)R_2Co_4O_{15}$ ($x = 1, 2$) (R = lanthanides)

W. Wong-Ng,[1,a)] G. Liu,[2] Y.G. Yan,[3] and J.A. Kaduk[4]
[1]*Materials Measurement Science Division, NIST, Gaithersburg, Maryland 20899*
[2]*Beijing National Laboratory for Condensed Matter Physics, Institute of Physics, Chinese Academy of Sciences, Beijing 100190, People's Republic of China*
[3]*State Key Laboratory of Advanced Technology for Materials Synthesis and Processing, Wuhan University of Technology, Wuhan, Hubei 430070, People's Republic of China*
[4]*BCPS, Illinois Institute of Technology, Chicago, Illinois 60616*

(Received 16 October 2012; accepted 4 February 2013)

The structure and X-ray patterns of two series of barium lanthanide cobaltates, namely, $Ba_4Sr_2R_2Co_4O_{15}$ (R = La, Nd, Sm, Eu, Gd, and Dy), and $Ba_5SrR_2Co_4O_{15}$ (R = La, Nd, Sm, Eu, and Gd) have been determined. These compounds crystallize in the space group $P6_3mc$; the unit-cell parameters of $Ba_4Sr_2R_2Co_4O_{15}$ (R from La to Dy) decrease from $a = 11.6128(2)$ Å to 11. 5266(9) Å, $c = 6.869\,03(11)$ to 6. 7630(5) Å, and $V = 802.23(3)$ Å^3 to 778.17(15) Å^3, respectively. In the $Ba_5SrR_2Co_4O_{15}$ series (R = La to Gd), the unit-cell parameters decrease from $a = 11.735\,44(14)$ Å to 11.619 79(12) Å, $c = 6.942\,89$ (14) Å to 6.836 52(8) Å, and $V = 828.08(3)$ Å^3 to 799.40(2) Å^3. In the general structure of $(Ba_{6-x}Sr_x)R_2Co_4O_{15}$, there are four Co ions per formula unit occupying one CoO_6 octahedral and three CoO_4 tetrahedral units. Through corner-sharing of these polyhedra, a larger Co_4O_{15} unit is formed. Sr^{2+} ions adopt both octahedral and 8-fold coordination environment. R^{3+} ions adopt 8-fold coordination (mixed site with Sr), while the larger Ba^{2+} ions assume both 10- and 11-fold coordination environments. The samples were found to be insulators. X-ray diffraction patterns of these samples have been determined and submitted to the Powder Diffraction File (PDF). © *2013 International Centre for Diffraction Data*. [doi:10.1017/S0885715613000171]

Key words: X-ray reference diffraction patterns, $(Ba_{6-x}Sr_x)R_2Co_4O_{15}$ ($x = 1, 2$) (R = La, Nd, Sm, Eu, and Gd), crystal structure

I. INTRODUCTION

Continuing demands for environmentally friendly alternative-energy technologies have led to increased activities in the area of thermoelectric (TE) research. For high-temperature waste-heat conversion applications, low-dimensional layered oxides have been found to have relatively high efficiency. The efficiency and performance of TE energy conversion or cooling is related to the dimensionless figure of merit (ZT) of the TE materials, given by $ZT = S^2\sigma T/\kappa$, where T is the absolute temperature, S is the Seebeck coefficient or TE power, σ is the electrical conductivity, and k is the thermal conductivity (Nolas *et al.*, 2001). Examples of these oxides include $NaCoO_x$ (Terasaki *et al.*, 1997), $Ca_2Co_3O_6$ (Mikami *et al.*, 2003; Mikami and Funahashi, 2005), and $Ca_3Co_4O_9$ (Masset *et al.*, 2000; Minami *et al.*, 2002; Grebille *et al.*, 2004; Hu *et al.*, 2005). Among these materials, the most efficient material, $Ca_3Co_4O_9$, is a misfit layered oxide that has two monoclinical subsystems with identical a, c, β, but different b (Masset *et al.*, 2000). However, to have materials with high enough efficiency for large-scale industrial applications, ZT of two or higher is a requirement.

The search for cobaltate compounds with improved TE properties continues worldwide. The goal of this paper is two-fold. Firstly, $(Ba_{6-x}Sr_x)R_2Co_4O_{15}$ ($x = 1, 2$) compounds are investigated for their structures. The structures of $Ba_6La_2Co_4O_{15}$ and $Ba_5CaNd_2Co_4O_{15}$ have been reported by Mevs and Müller-Buschbaum (1990a), and Müller-Buschbaum and Martin (1992). Since X-ray diffraction is a non-destructive technique for phase identification, X-ray diffraction patterns are especially important for phase characterization, therefore another goal of this investigation was to determine the experimental patterns for $Ba_4Sr_2R_2Co_4O_{15}$ (R = La, Nd, Sm, Gd, and Dy), and $Ba_5SrR_2Co_4O_{15}$ (R = La, Nd, Sm, Eu, and Gd), and to make them widely available through submission to the Powder Diffraction File (PDF) (ICDD).

II. EXPERIMENTAL

A. Sample preparation

All samples were prepared by heating a stoichiometric mixture of $BaCO_3$, R_2O_3 (R = La, Nd, Sm, Eu, Gd, Dy, Ho, Y, Er, Tm, Yb, and Lu), and Co_3O_4 in air. La_2O_3 and Nd_2O_3 were first heat treated at 550 °C overnight prior to use to ensure the absence of carbonates and hydroxides. Samples were weighed, well-mixed, and calcined at 800 °C for one day, 950 °C for one day, and subsequently at 980 °C, with intermediate grindings and pelletizations, for another 6 days. During each heat treatment, all samples were furnace cooled. The phase purity of the samples was established by powder X-ray diffraction.

[a)] Author to whom correspondence should be addressed. Electronic mail: winnie.wong-ng@nist.gov

0885-7156/2013/28(3)/212/10/$18.00

B. X-ray Rietveld refinements and powder reference patterns

The $Ba_4Sr_2R_2Co_4O_{15}$ (R = La, Nd, Sm, Eu, and Gd) and $Ba_5SrR_2Co_4O_{15}$ (R = La, Nd, Sm, Eu, Gd, and Dy) powders were mounted as ethanol slurries on zero-background cells. The X-ray powder patterns of the former samples were measured on a Bruker D2 Phaser diffractometer. The X-ray powder patterns of the latter group of samples were measured at ambient conditions on a Panalytical X'Pert Pro MPD diffractometer equipped with a PIXcel position-sensitive detector and an Anton Paar HTK1200N furnace. Patterns were measured (Cu$K\alpha$ radiation, 45 kV, 40 mA, 0.5° divergence slit, and 0.02 rad Soller slits) from 5 to 130°2θ in 0.02° steps.

The Rietveld refinement technique (Rietveld, 1969) with the software suite GSAS (Larson and von Dreele, 2004) was used to determine the structure of $(Ba_{6-x}Sr_x)R_2Co_4O_{15}$. A structural model of $Ba_5SrPr_2Co_4O_{15}$ reported previously (Müller-Buschbaum and Uensal, 1996) was used for structural refinements. Reference patterns were obtained with a Rietveld pattern decomposition technique. Using this technique, the reported peak positions were derived from the extracted integrated intensities, and positions calculated from the unit-cell parameters. When peaks are not resolved at the resolution function, the intensities are summed, and an intensity-weighted d-spacing is reported. They are also corrected for systematic errors both in d-spacing and intensity. In summary, these patterns represent ideal specimen patterns.

C. Bond valence sum (V_b) calculation

The bond valence sum values, V_b, for the Ba, R, and Co sites were calculated using the Brown–Altermatt empirical expression (Brown and Altermatt, 1985; Brese and O'Keeffe, 1991). The V_b of an atom i is defined as the sum of the bond valences v_{ij} of all the bonds from atoms i to atoms j. The most commonly adopted empirical expression for bond valence v_{ij} as a function of the interatomic distance d_{ij} is $v_{ij} = \exp[(R_0 - d_{ij})/B]$. The parameter, B, is commonly taken to be a "universal" constant equal to 0.37 Å. The values for the reference distance R_0 (Å) for Ba–O, Sr–O, Co^{2+}–O, Co^{3+}–O, La–O, Nd–O, Sm–O, Eu–O, Gd–O, and Dy–O are 2.29, 2.118, 1.692, 1.70, 2.172, 2.117, 2.088, 2.076, 2.065, and 2.036, respectively (Brown and Altermatt, 1985; Brese and O'Keeffe, 1991).

III. RESULTS AND DISCUSSION

Phases for $Ba_4Sr_2R_2Co_4O_{15}$, and $Ba_5SrR_2Co_4O_{15}$ were successfully prepared only for compounds with relatively larger size of R. Based on X-ray diffraction results, in $Ba_4Sr_2R_2Co_4O_{15}$, compounds with R = Dy, Ho, Er, Yb, Tm, and Lu, and in $Ba_5SrR_2Co_4O_{15}$, compounds with R = Ho,

TABLE I. Refinement residuals and phases present for (a) $Ba_4Sr_2R_2Co_4O_{15}$ and (b) $Ba_5SrR_2Co_4O_{15}$. Values inside brackets are standard deviations.

(a) $Ba_4Sr_2R_2Co_4O_{15}$						
R	La	Nd	Sm	Eu	Gd	Dy
R_{wp}	0.0688	0.0116	0.0293	0.0258	0.0257	0.0226
Rp	0.0458	0.0088	0.0220	0.0195	0.0194	0.0177
χ^2	2.354	2.990	2.056	2.238	2.231	2.497
$R(F)$	0.0401	0.0300	0.1159	0.0782	0.0708	0.1059
$R(F^2)$	0.0705	0.0745	0.1728	0.1291	0.1176	0.1575
$\Delta F(+)$, eÅ^{-3}	4.0	1.52	6.36	3.79	3.35	4.06
$\Delta F(-)$, eÅ^{-3}	−6.6	−1.43	−6.15	−2.87	−2.60	−7.10
Impurities (% mass fraction)						
(Ba,Sr)CoO_4	–	4.1(1)	–	–	–	15.9(4)
R_2O_3	–	0.7(1)	–	–	–	–
$BaSrCo_2O_6$	–	0.7(1)	–	–	–	–
CoO	–	1.2(1)	–	–	–	–
$BaCoO_x$	0.1(1)	–	–	–	–	–
BaR_2O_4	1.2(1)	–	–	–	–	–
Ba_2CoO_4	6.9(1)	–	–	–	–	–
(b) $Ba_5SrR_2Co_4O_{15}$						
Rwp	0.1249	0.0654	0.0582	0.0767	0.0498	
Rp	0.0972	0.0496	0.0451	0.0598	0.0386	
$\chi 2$	1.492	2.429	2.265	1.527	1.712	
$R(F)$	0.0585	0.0268	0.0240	0.0299	0.0251	
$R(F^2)$	0.0985	0.0492	0.0451	0.0538	0.0440	
DF(+), eÅ^{-3}	4.2	1.9	1.9	2.2	2.2	
DF(−), eÅ^{-3}	−2.6	−1.9	−2.2	−3.1	−2.3	
Impurities (% mass fraction)						
(Ba, Sr)CoO_3	0.6(1)	0.2(1)	2.9(1)	4.9(1)	3.5(1)	
$BaCO_3$	0.5(1)	2.1(1)	1.6(1)	1.6(1)	1.9(1)	
$BaR2CoO_5$	0.3(1)	1.6(1)	–	–	–	
$BaCoOx$	0.3(1)	2.1(1)	0.6(1)	1.1(1)	0.5(1)	
BaR_2O_4	–	2.1(1)	–	–	–	
R_2O_3	–	–	0.6(1)	0.5(1)	0.7(1)	

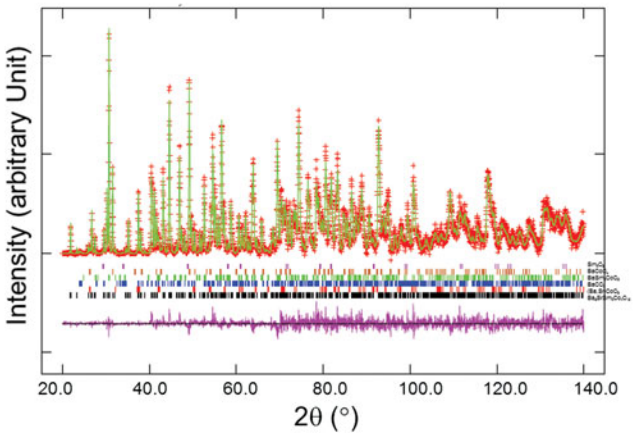

Figure 1. Observed (crosses), calculated (solid line), and difference XRD pattern (bottom) for $Ba_5SrSm_2Co_4O_{15}$ by Rietveld analysis technique. The difference pattern is plotted at the same scale as the other patterns up to 70° 2θ. At higher 2θ angles, the scale has been magnified five times. Phases present are indicated next to the rows of tick marks (from bottom to top: $Ba_5SrSm_2Co_4O_{15}$, (Ba, Sr)CoO_3, $BaCO_3$, $BaSm_2CoO_5$, $BaCoO_x$, and Sm_2O_3).

Er, Yb, Tm, and Lu cannot be made at all under the current synthesis conditions. X-ray diffraction data of each $Ba_4Sr_2R_2Co_4O_{15}$ and $Ba_5SrR_2Co_4O_{15}$ were indexable with a hexagonal unit cell and with a space group of $P6_3mc$ (No. 186). X-ray patterns of the composition of the Ho-analog, $Ba_4Sr_2Ho_2Co_4O_{15}$, indicate a different structure. The major product of this preparation has the $P4mm$ SrHoO3 type structure, with $a = 4.1301(1)$, $c = 4.1430(2)$ Å, and $V = 70.670(5)$ Å^3. Refinement of this structure indicated that the A site was occupied by Sr, and that the oxygen sites were fully occupied. This sample contains 5.9(1)% mass fraction of $BaSrHo_4O_8$, 3.4(1)% mass fraction of $CaCoO_{2+x}$, and 0.8(1)% mass fraction of a spinel, and traces of additional phases.

The samples are essentially isolators as they are very resistive and no reasonable Seebeck coefficient signal could be obtained.

A. Structure of $Ba_{6-x}(Sr,Ca)_xR_2Co_4O_{15}$

Table I gives the refinement residuals for $Ba_4Sr_2R_2Co_4O_{15}$ and $Ba_5SrR_2Co_4O_{15}$. Figure 1 provides the

TABLE II. Unit cell parameters of $Ba_4Sr_2R_2Co_4O_{15}$ and $Ba_5SrR_2Co_4O_{15}$ ($P6_3mc$ (No. 186), $Z = 2$), D_x refers to calculated density. Values inside brackets are standard deviations.

Compounds	a (Å)	c (Å)	V(Å^3)	D_x (g cm^{-3})	$r(R^{3+})$ (VIII-coord)
$Ba_4Sr_2La_2Co_4O_{15}$	11.7022(1)	6.908 36(8)	819.30(2)	5.991	1.160
$Ba_4Sr_2Nd_2Co_4O_{15}$	11.6457(2)	6.861 45(11)	805.90(3)	6.135	1.109
$Ba_4Sr_2Sm_2Co_4O_{15}$	11.6121(8)	6.8392(5)	798.66(14)	6.242	1.079
$Ba_4Sr_2Eu_2Co_4O_{15}$	11.5940(4)	6.8210(2)	794.05(6)	6.291	1.066
$Ba_4Sr_2Gd_2Co_4O_{15}$	11.5872(4)	6.8169(2)	792.63(6)	6.342	1.053
$Ba_4Sr_2Dy_2Co_4O_{15}$	11.5266(9)	6.7630(5)	778.2(2)	6.508	1.027
$Ba_5SrLa_2Co_4O_{15}$	11.7354(2)	6.942 89(14)	828.08(3)	6.127	1.160
$Ba_5SrNd_2Co_4O_{15}$	11.672 18(12)	6.886 89(8)	812.56(2)	6.288	1.109
$Ba_5SrSm_2Co_4O_{15}$	11.640 12(12)	6.860 26(8)	804.98(2)	6.398	1.079
$Ba_5SrEu_2Co_4O_{15}$	11.6250(2)	6.841 91(12)	800.75(3)	6.445	1.066
$Ba_5SrGd_2Co_4O_{15}$	11.619 79(12)	6.836 52(8)	799.40(2)	6.500	1.053

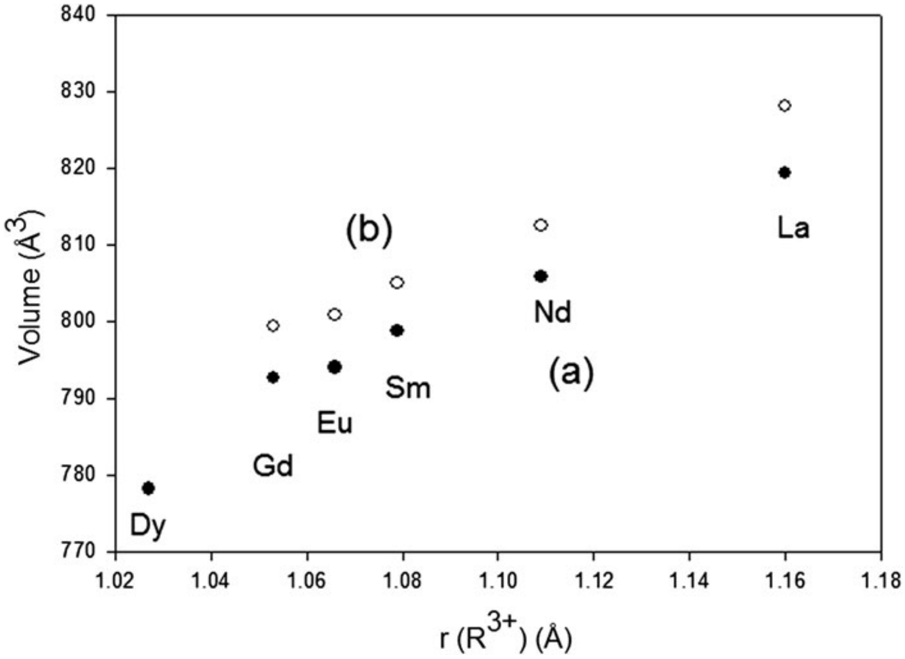

Figure 2. Plot of unit-cell volume of (a) $Ba_4Sr_2R_2Co_4O_{15}$ and (b) $Ba_5SrR_2Co_4O_{15}$ vs. $r(R^{3+})$ [where "r" is the Shannon Ionic Radii (1976)].

TABLE III(a). Atomic coordinates and isotropic displacement factors for $Ba_4Sr_2R_2Co_4O_{15}$; values inside brackets are standard deviations.

Atom	x	y	z	Occupied	U_{iso}	Site
(i) R = La						
Sr1	0.0	0.0	−0.0048	1.0	0.0055(2)	2a
Ba2	0.174 78(6)	0.825 22(6)	0.1700(5)	1.0	0.0055(2)	6c
Ba3	0.333 33	0.666 67	0.4801(5)	1.0	0.0055(2)	2b
Sr4	0.475 99(6)	0.524 01(6)	0.8255(4)	0.333 33	0.0055(2)	6c
La5	0.475 99(6)	0.524 01(6)	0.8255(4)	0.666 67	0.0055(2)	6c
Co6	0.333 33	0.666 67	−0.0079(9)	1.0	0.0035(2)	2b
Co7	0.175 15(14)	0.824 85(14)	0.6544(7)	1.0	0.0035(2)	6c
O8	0.6684(6)	0.0733(6)	0.0280(9)	1.0	0.01	12d
O9	0.2465(3)	0.7535(3)	0.8397(11)	1.0	0.01	6c
O10	0.4130(3)	0.5870(3)	0.1502(11)	1.0	0.01	6c
O11	0.9053(4)	0.0947(4)	0.2491(12)	1.0	0.01	6c
(ii) R = Nd						
Sr1	0.0	0.0	0.0	1.0	0.0157(4)	2a
Ba2	0.174 53(8)	0.825 47(8)	0.1757(6)	1.0	0.0157(4)	6c
Ba3	0.333 33	0.666 67	0.4875(6)	1.0	0.0157(4)	2b
Sr4	0.476 17(7)	0.523 83(7)	0.8320(6)	0.333 33	0.0103(5)	6c
Nd5	0.476 17(7)	0.523 83(7)	0.8320(6)	0.666 67	0.0103(5)	6c
Co6	0.333 33	0.666 67	−0.0101(10)	1.0	0.0090(8)	2b
Co7	0.1759(2)	0.8241(2)	0.6563(10)	1.0	0.0090(8)	6c
O8	0.6658(6)	0.0673(6)	0.0306(10)	1.0	0.01	12d
O9	0.2469(3)	0.7531(3)	0.8387(13)	1.0	0.01	6c
O10	0.4105(4)	0.5895(4)	0.1618(14)	1.0	0.01	6c
O11	0.9040(4)	0.0960(4)	0.2571(14)	1.0	0.01	6c
(iii) R = Sm						
Sr1	0.0	0.0	0.0	1.0	0.01	2a
Ba2	0.1742(2)	0.8259(2)	0.179(2)	1.0	0.01	6c
Ba3	0.333 33	0.666 67	0.498(2)	1.0	0.01	2b
Sr4	0.4763(2)	0.5237(2)	0.833(2)	0.333 33	0.01	6c
Sm5	0.4763(2)	0.5237(2)	0.833(2)	0.666 67	0.01	6c
Co6	0.333 33	0.666 67	−0.032(2)	1.0	0.01	2b
Co7	0.1763(4)	0.8237(4)	0.651(2)	1.0	0.01	6c
O8	0.6553(7)	0.0789(8)	0.039(2)	1.0	0.01	12d
O9	0.2424(3)	0.7576(3)	0.842(2)	1.0	0.01	6c
O10	0.4107(4)	0.5893(4)	0.148(2)	1.0	0.01	6c
O11	0.9067(5)	0.0933(5)	0.256(2)	1.0	0.01	6c
(iv) R = Eu						
Sr1	0.0	0.0	0.0	1.0	0.018 16	2a
Ba2	0.1744(2)	0.8256(2)	0.1788(13)	1.0	0.018 16	6c
Ba3	0.333 33	0.666 67	0.4936(11)	1.0	0.018 16	2b
Sr4	0.475 78(14)	0.524 22(14)	0.8338(12)	0.333 33	0.005 05	6c
Eu5	0.475 78(14)	0.524 22(14)	0.8338(12)	0.666 67	0.005 05	6c
Co6	0.333 33	0.666 67	−0.0226(14)	1.0	0.005	2b
Co7	0.1759(3)	0.8241(3)	0.654(2)	1.0	0.005	6c
O8	0.6569(6)	0.0766(8)	0.0406(15)	1.0	0.01	12d
O9	0.2459(3)	0.7541(3)	0.837(2)	1.0	0.01	6c
O10	0.4111(4)	0.5889(4)	0.153(2)	1.0	0.01	6c
O11	0.9061(5)	0.0939(5)	0.258(2)	1.0	0.01	6c
(v) R = Gd						
Sr1	0.0	0.0	0.0	1.0	0.0131(8)	2a
Ba2	0.1744(2)	0.8256(2)	0.1785(13)	1.0	0.0131(8)	6c
Ba3	0.333 33	0.666 67	0.4937(12)	1.0	0.0131(8)	2b
Sr4	0.475 82(15)	0.524 17(15)	0.8337(12)	0.333 33	0.0064(10)	6c
Gd5	0.475 82(15)	0.524 17(15)	0.8337(12)	0.666 67	0.0064(10)	6c
Co6	0.333 33	0.666 67	−0.0219(15)	1.0	0.005	2b
Co7	0.1761(3)	0.8239(3)	0.654(2)	1.0	0.005	6c
O8	0.6568(7)	0.0768(8)	0.040(2)	1.0	0.019(4)	12d
O9	0.2463(3)	0.7537(3)	0.836(2)	1.0	0.019(4)	6c
O10	0.4110(4)	0.5890(4)	0.154(2)	1.0	0.019(4)	6c
O11	0.9060(5)	0.0940(5)	0.257(2)	1.0	0.019(4)	6c
(vi) R = Dy						
Sr1	0.0	0.0	0.0	1.0	0.013 14	2a
Ba2	0.1734(4)	0.8266(4)	0.178(3)	1.0	0.013 14	6c
Ba3	0.333 33	0.666 67	0.486(2)	1.0	0.013 14	2b
Sr4	0.4742(3)	0.5258(3)	0.839(2)	0.333 33	0.006 43	6c
Dy5	0.4742(3)	0.5258(3)	0.839(2)	0.666 67	0.006 43	6c

Continued

TABLE III(a). Continued

Atom	x	y	z	Occupied	U_{iso}	Site
Co6	0.333 33	0.666 67	0.018(2)	1.0	0.005	2b
Co7	0.1837(5)	0.8163(5)	0.668(3)	1.0	0.005	6c
O8	0.6516(8)	0.0802(9)	0.042(3)	1.0	0.019 25	12d
O9	0.2636(4)	0.7364(4)	0.820(3)	1.0	0.019 25	6c
O10	0.4125(4)	0.5875(4)	0.177(3)	1.0	0.019 25	6c
O11	0.9031(6)	0.0969(6)	0.251(2)	1.0	0.019 25	6c

Rietveld refinement results for $Ba_5SrSm_2Co_4O_{15}$ as an example. The observed (crosses), calculated (solid line), and difference XRD patterns (bottom) for $Ba_5SrSm_2Co_4O_{15}$, as determined by the Rietveld analysis technique, are shown. The difference pattern is plotted at the same scale as the other patterns up to 70°2θ. At higher 2θ angles, the scale has been magnified five times. The rows of tick marks refer to the calculated peak positions. The refinement residuals mainly reflect variations in the counting times, and the presence of traces of additional impurities as indicated.

Table II lists the unit-cell parameters for $Ba_4Sr_2R_2Co_4O_{15}$ and $Ba_5SrR_2Co_4O_{15}$. The calculated density values, D_x, in both series increase as the size of R decreases. Figure 2 gives the plot of the unit-cell volumes, V, of $Ba_4Sr_2R_2Co_4O_{15}$ and $Ba_5SrR_2Co_4O_{15}$ vs. Shannon ionic radius, $r(R^{3+})$. The unit-cell volume decreases across the lanthanide series from La to Dy,

TABLE III(b). Atomic coordinates and isotropic displacement factors for $Ba_5SrR_2Co_4O_{15}$. Values inside brackets are standard deviations.

Atom	x	y	z	Occupied	U_{iso}	Site
(i) R = La						
Ba1/Sr2	0.0	0.0	−0.0048	0.5/0.5	0.0067(4)	2a
Ba3	0.174 56(11)	0.825 44(11)	0.1617(8)	1.0	0.0067(4)	6c
Ba5	0.333 33	0.666 67	0.4745(8)	1.0	0.0067(4)	2b
Ba7	0.475 84(11)	0.524 16(11)	0.8164(7)	0.166 67	0.0067(4)	6c
Sr8	0.475 84(11)	0.524 16(11)	0.8164(7)	0.166 67	0.0067(4)	6c
La9	0.475 84(11)	0.524 16(11)	0.8164(7)	0.666 67	0.0067(4)	6c
Co10	0.333 33	0.666 67	−0.0431(10)	1.0	0.0046(4)	2b
Co11	0.177 35(25)	0.822 65(25)	0.6374(11)	1.0	0.0046(4)	6c
O12	0.6609(5)	0.0800(6)	0.0241(11)	1.0	0.01	12d
O13	0.242 42(25)	0.757 58(25)	0.8301(12)	1.0	0.01	6c
O14	0.412 54(28)	0.587 45(28)	0.1238(11)	1.0	0.01	6c
O15	0.9005(4)	0.0995(4)	0.2504(14)	1.0	0.01	6c
(ii) R = Nd						
Ba1/Sr2	0.0	0.0	−0.0048	0.5/0.5	0.004 13(17)	2a
Ba3	0.174 70(6)	0.825 30(6)	0.1558(5)	1.0	0.004 13(17)	6c
Ba5	0.333 33	0.666 67	0.4669(5)	1.0	0.004 13(17)	2b
Ba7	0.475 66(6)	0.524 34(6)	0.8150(4)	0.166 67	0.004 13(17)	6c
Sr8	0.475 66(6)	0.524 34(6)	0.8150(4)	0.166 67	0.004 13(17)	6c
Nd9	0.475 66(6)	0.524 34(6)	0.8150(4)	0.666 67	0.004 13(17)	6c
Co10	0.333 33	0.666 67	−0.0126(9)	1.0	0.002 11(17)	2b
Co11	0.176 95(15)	0.823 05(15)	0.6457(8)	1.0	0.002 11(17)	6c
O12	0.6663(6)	0.0705(6)	0.0195(9)	1.0	0.01	12d
O13	0.250 53(29)	0.749 47(29)	0.8248(11)	1.0	0.01	6c
O14	0.413 57(32)	0.586 42(32)	0.1403(12)	1.0	0.01	6c
O15	0.9030(4)	0.0970(4)	0.2462(13)	1.0	0.01	6c
(iii) R = Sm						
Ba1/Sr2	0.0	0.0	−0.0048	0.5/0.5	0.006 73(16)	2a
Ba3	0.174 92(6)	0.825 08(6)	0.1533(4)	1.0	0.006 73(16)	6c
Ba5	0.333 33	0.666 67	0.4660(4)	1.0	0.006 73(16)	2b
Ba7	0.475 73(5)	0.524 27(5)	0.8167(4)	0.166 67	0.006 73(16)	6c
Sr8	0.475 73(5)	0.524 27(5)	0.8167(4)	0.166 67	0.006 73(16)	6c
Sm9	0.475 73(5)	0.524 27(5)	0.8167(4)	0.666 67	0.006 73(16)	6c
Co10	0.333 33	0.666 67	−0.0071(8)	1.0	0.004 72(16)	2b
Co11	0.176 54(14)	0.823 46(14)	0.6490(8)	1.0	0.004 72(16)	6c
O12	0.6672(5)	0.0708(6)	0.0193(8)	1.0	0.0032(13)	12d
O13	0.251 74(27)	0.748 26(27)	0.8267(11)	1.0	0.0032(13)	6c
O14	0.413 78(30)	0.586 22(30)	0.1418(11)	1.0	0.0032(13)	6c
O15	0.902 40(34)	0.097 60(34)	0.2519(12)	1.0	0.0032(13)	6c
(iv) R = Eu						
Ba1/Sr2	0.0	0.0	−0.0048	0.5/0.5	0.0065(2)	2a
Ba3	0.174 41(8)	0.825 59(8)	0.1560(6)	1.0	0.0065(2)	6c
Ba5	0.333 33	0.666 67	0.4711(5)	1.0	0.0065(2)	2b

Continued

TABLE III(b). Continued

Atom	x	y	z	Occupied	U_{iso}	Site
Ba7	0.475 59(8)	0.52441(8)	0.8168(5)	0.166 67	0.0065(2)	6c
Sr8	0.475 59(8)	0.52441(8)	0.8168(5)	0.166 67	0.0065(2)	6c
Eu9	0.475 59(8)	0.52441(8)	0.8168(5)	0.666 67	0.0065(2)	6c
Co10	0.333 33	0.666 67	−0.0264(9)	1.0	0.0045(2)	2b
Co11	0.176 93(18)	0.823 07(18)	0.6401(9)	1.0	0.0045(2)	6c
O12	0.6625(5)	0.0753(6)	0.0212(9)	1.0	0.01	12d
O13	0.250 57(24)	0.749 43(24)	0.8176(10)	1.0	0.01	6c
O14	0.410 90(28)	0.589 10(28)	0.1380(10)	1.0	0.01	6c
O15	0.901 80(34)	0.098 20(34)	0.2509(13)	1.0	0.01	6c
(v) $R=$Gd						
Ba1/Sr2	0.0	0.0	−0.0048	0.5/0.5	0.008 39(18)	2a
Ba3	0.174 81(6)	0.825 19(6)	0.1552(4)	1.0	0.008 39(18)	6c
Ba5	0.333 33	0.666 67	0.4687(4)	1.0	0.008 39(18)	2b
Ba7	0.475 55(6)	0.524 45(6)	0.8185(4)	0.166 67	0.008 39(18)	6c
Sr8	0.475 55(6)	0.524 45(6)	0.8185(4)	0.166 67	0.008 39(18)	6c
Gd9	0.475 55(6)	0.524 45(6)	0.8185(4)	0.666 67	0.008 39(18)	6c
Co10	0.333 33	0.666 67	−0.0136(8)	1.0	0.006 37(18)	2b
Co11	0.176 87(14)	0.823 13(14)	0.6455(8)	1.0	0.006 37(18)	6c
O12	0.6648(5)	0.0698(5)	0.0214(8)	1.0	0.01	12d
O13	0.252 48(24)	0.747 52(24)	0.8213(10)	1.0	0.01	6c
O14	0.412 47(28)	0.587 53(28)	0.1416(10)	1.0	0.01	6c
O15	0.902 24(32)	0.097 76(32)	0.2513(11)	1.0	0.01	6c

or with the decreasing size of the ionic radius (Shannon, 1976) (lanthanide contraction) of the metal ion at the octahedral site. This decreasing volume is a result of the decrease in both the *a*- and the *c*-parameters.

The atomic coordinates, displacement parameters for the structures of $Ba_4Sr_2R_2Co_4O_{15}$ and $Ba_5SrR_2Co_4O_{15}$ are given in Tables III(a) and 3(b). $Ba_4Sr_2R_2Co_4O_{15}$ and $Ba_5SrR_2Co_4O_{15}$ are isostructural with $Ba_6R_2Fe_4O_{15}$ (Rüter and Müller-Buschbaum, 1990; Mevs and Müller-Buschbaum, 1990b, 1990c, 1992; Abe *et al.*, 2006). The structure of $Ba_{6-x}Sr_xR_2Co_4O_{15}$ in general consists of two crystallographically independent Co sites, one is 6-fold, while the other is 4-fold coordinated. The CoO_6 octahedra and CoO_4 tetrahedra are linked by corner-shared oxygen ions. Specifically, a CoO_6 octahedron in the center can be viewed as sharing three corners of its triangular face with three tetrahedral CoO_4 units, leading to a Co_4O_{15} cluster (Figure 3). In $Ba_4Sr_2R_2Co_4O_{15}$, all R sites are mixed with Sr (randomly occupied by 2/3R and 1/3Sr), while in $Ba_5SrR_2Co_4O_{15}$, all R sites are mixed with Ba and Sr (randomly occupied by 2/3R, 1/6Ba, and 1/6Sr). Figure 4 gives the structure of $(Ba_{6-x}Sr_x)R_2Co_4O_{15}$ as viewed along the *c*-axis. It features six units of Co_4O_{15} and seven SrO_6 octahedral units viewed along the *b*-axis. For clarity,

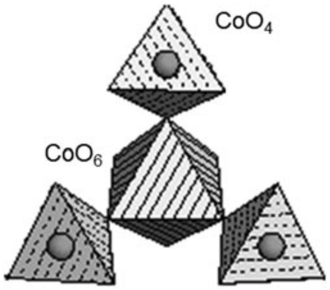

Figure 3. The structure motif of Co_4O_{15} which consists of three corner-shared [CoO_4] tetrahedral units with one CoO_6 octahedral unit at the center.

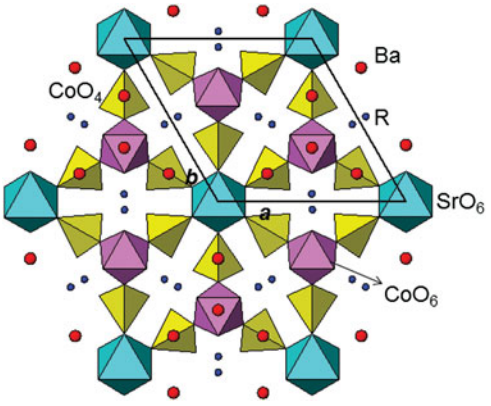

Figure 4. Crystal structure of $Ba_4Sr_2R_2Co_4O_{15}$ at room temperature showing the unit cell outline, and different coordination environment of tetrahedral [CoO_4] and octahedral [CoO_6] units. The 8-fold coordinated (R, Sr)O_8 bisdisphenoids and BaO_{10} and BaO_{12} polyhedra were not shown for clarity.

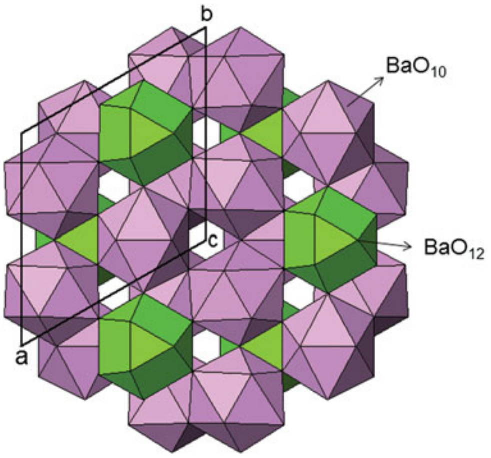

Figure 5. Crystal structure of $Ba_4Sr_2Gd_2Co_4O_{15}$ at room temperature showing the capped trigonal prism BaO_{10} and cubic close packed BaO_{12} coordination environment.

TABLE IV(a). Bond distances and bond valence sum values (V_b) for $Ba_4Sr_2R_2Co_4O_{15}$. Values inside brackets are standard deviations.

Atom	Atom	Distances	V_b
(i) R = La			
Sr1	O11	2.601(8) × 3	1.710
		2.565(7) × 3	
Ba2	O8	2.970(6) × 2	1.772
		2.952(6) × 2	
	O9	2.706(8)	
	O10	2.7866(10) × 2	
	O11	3.120(2) × 2	
		3.330(9)	
Ba3	O8	3.072(6) × 6	1.886
	O9	3.044(7) × 3	
	O10	2.793(7) × 3	
La5/Sr4	O8	2.582(6) × 2	3.002
		2.418(5) × 2	
	O9	2.5256(12) × 2	
	O10	2.581(7)	
		2.555(7)	
Co6	O9	2.051(6) × 3	2.692
	O10	1.949(7) × 3	
Co7	O8	1.831(5) × 2	2.799
	O9	1.931(6)	
	O11	1.756(7)	
(ii) R = Nd			
Sr1	O11	2.619(9) × 3	1.695
		2.555(8) × 3	
Ba2	O8	2.910(7) × 2	1.851
		2.937(7) × 2	
	O9	2.735(9)	
	O10	2.7761(14) × 2	
	O11	3.104(2) × 2	
		3.280(10)	
Ba3	O8	3.107(6) × 6	1.953
	O9	2.974(9) × 3	
	O10	2.723(9) × 3	
Nd5/Sr4	O8	2.586(6) × 2	2.842
		2.359(6) × 2	
	O9	2.5140(14) × 2	
	O10	2.622(9)	
		2.567(8)	
Co6	O9	2.029(7) × 3	2.747
	O10	1.953(8) × 3	
Co7	O8	1.847(6) × 2	2.788
	O9	1.902(7)	
	O11	1.754(7)	
(iii) R = Sm			
Sr1	O11	2.564(13) × 3	1.930
		2.513(10) × 3	
Ba2	O8	3.071(8) × 2	1.706
		3.004(9) × 2	
	O9	2.684(11)	
	O10	2.781(4) × 2	
	O11	3.081(2) × 2	
		3.32(2)	
Ba3	O8	2.904(8) × 6	2.263
	O9	2.980(9) × 3	
	O10	2.852(10) × 3	
Sm5/Sr4	O8	2.439(7) × 2	3.088
		2.325(7) × 2	
	O9	2.522(4) × 2	
	O10	2.528(10)	
		2.599(9)	
Co6	O9	2.021(7) × 3	2.641
	O10	1.987(7) × 3	
Co7	O8	1.864(6) × 2	2.651
	O9	1.865(8)	
	O11	1.818(8)	
(iv) R = Eu			
Sr1	O11	2.577(12) × 3	1.913
		2.508(9) × 3	
Ba2	O8	3.028(8) × 2	1.711
		2.998(8) × 2	
	O9	2.739(10)	
	O10	2.770(3) × 2	
	O11	3.083(3) × 2	
		3.296(15)	
Ba3	O8	2.939(8) × 6	2.332
	O9	2.926(9) × 3	
	O10	2.800(9) × 3	
Eu5/Sr4	O8	2.444(7) × 2	3.027
		2.336(7) × 2	
	O9	2.499(3) × 2	
	O10	2.535(10)	
		2.584(8)	
Co6	O9	2.001(7) × 3	2.780
	O104	1.969(8) × 3	
Co7	O8	1.858(6) × 2	2.709
	O9	1.877(7)	
	O11	1.790(8)	
(v) R = Gd			
Sr1	O11	2.573(12) × 3	1.914
		2.511(9) × 3	
Ba2	O8	3.029(8) × 2	1.713
		2.996(8) × 2	
	O9	2.744(10)	
	O10	2.768(3) × 2	
	O11	3.080(3) × 2	
		3.296(15)	
Ba3	O8	2.934(8) × 6	2.378
	O9	2.916(9) × 3	
	O10	2.792(9) × 3	
Gd5/Sr4	O8	2.442(7) × 2	2.983
		2.333(7) × 2	
	O9	2.497(3) × 2	
	O10	2.541(10)	
		2.581(8)	
Co6	O9	1.997(7) × 3	2.806
	O10	1.966(8) × 3	
Co7	O8	1.857(6) × 2	2.714
	O9	1.876(7)	
	O11	1.790(8)	
(vi) R = Dy			
Sr1	O11	2.576(14) × 3	1.769
		2.564(12) × 3	
Ba2	O8	3.074(9) × 2	1.545
		3.019(10)	
	O9	3.018(13) × 2	
	O10	2.765(6) × 2	
	O11	3.046(6) × 2	
		3.26(2)	
Ba3	O8	2.859(9) × 6	3.642
	O9	2.650(11) × 3	
	O10	2.623(11) × 3	
Gd5/Sr4	O8	2.401(9) × 2	3.144
		2.296(9) × 2	
	O9	2.439(5) × 2	
	O10	2.598(12)	
		2.513(10)	
Co6	O9	1.929(8) × 3	3.307
	O10	1.912(8) × 3	
Co7	O8	1.867(6) × 2	2.577
	O9	1.899(9)	
	O11	1.822(9)	

TABLE IV(b). Bond distances and bond valence sum values (V_b) for $Ba_5SrR_2Co_4O_{15}$. Values inside brackets are standard deviations.

Atom	Atom	Distances	V_b
(i) $R = La$			
Ba1/Sr2	O15	2.689(10) × 3	1.777
		2.641(7) × 3	
Ba3	O12	3.083(7) × 2	1.624
		3.025(7) × 2	
	O13	2.684(8)	
	O14	2.807(2) × 2	
	O15	3.144(3) × 2	
		3.238(12)	
Ba5	O12	2.959(7) × 6	1.883
	O13	3.084(7) × 3	
	O14	2.919(7) × 3	
La9/Ba7/Sr8	O12	2.497(6) × 2	3.468
		2.407(5) × 2	
	O13	2.542(2) × 2	
	O14	2.492(7)	
		2.634(6)	
Co10	O13	2.047(5) × 3	2.567
	O14	1.984(6) × 3	
Co11	O12	1.833(5) × 2	2.844
	O13	1.881(6)	
	O15	1.767(6)	
(ii) $R = Nd$			
Ba1/Sr2	O15	2.615(9) × 3	2.053
		2.606(7) × 3	
Ba3	O12	2.929(7) × 2	1.768
		2.989(6) × 2	
	O13	2.747(8)	
	O14	2.7795(11) × 2	
	O15	3.128(2) × 2	
		3.228(10)	
Ba5	O12	3.087(6) × 6	1.974
	O13	2.980(8) × 3	
	O14	2.773(8) × 3	
Ba7/Sr8/Nd9	O12	2.556(6) × 2	3.134
		2.403(6) × 2	
	O13	2.5039(12) × 2	
	O14	2.568(8)	
		2.542(7)	
Co10	O13	2.014(6) × 3	2.878
	O14	1.934(7) × 3	
Co11	O12	1.836(5) × 2	2.772
	O13	1.933(6)	
	O15	1.758(7)	
(iii) $R = Sm$			
Ba1/Sr2	O15	2.641(8) × 3	2.061
		2.580(7) × 3	
Ba3	O12	2.915(6) × 2	1.832
		2.987(6) × 2	
	O13	2.724(7)	
	O14	2.7671(10) × 2	
	O15	3.135(2) × 2	
		3.164(9)	
Ba5	O12	3.081(6) × 6	2.043
	O13	2.972(7) × 3	
	O14	2.752(7) × 3	
Ba7/Sr8/Sm9	O12	2.563(6) × 2	3.037
		2.395(5) × 2	
	O13	2.4960(10) × 2	
	O14	2.556(7)	
		2.530(6)	
Co10	O13	2.001(6) × 3	2.999
	O14	1.917(6) × 3	
Co11	O12	1.837(5) × 2	2.792
	O13	1.945(6)	
	O15	1.741(6)	
(iv) $R = Eu$			
Ba1/Sr2	O15	2.640(9) × 3	2.037
		2.589(7) × 3	
Ba3	O12	2.986(6) × 2	1.716
		2.997(6) × 2	
	O13	2.777(7)	
	O14	2.7742(14) × 2	
	O15	3.118(2) × 2	
		3.168(10)	
Ba5	O12	2.995(6) × 6	2.308
	O13	2.898(7) × 3	
	O14	2.763(7) × 3	
Ba7/Sr8/La9	O12	2.504(6) × 2	3.107
		2.372(5) × 2	
	O13	2.4916(14) × 2	
	O14	2.555(7)	
		2.592(6)	
Co10	O13	1.979(5) × 3	3.044
	O14	1.925(6) × 3	
Co11	O12	1.826(4) × 2	2.836
	O13	1.917(5)	
	O15	1.757(6)	
(iv) $R = Gd$			
Ba1/Sr2	O15	2.634(8) × 3	2.082
		2.579(6) × 3	
Ba3	O12	2.910(6) × 2	1.807
		2.993(6) × 2	
	O13	2.767(7)	
	O14	2.7646(10) × 2	
	O15	3.124(2) × 2	
		3.167(8)	
Ba5	O12	3.072(6) × 6	2.164
	O13	2.908(7) × 3	
	O14	2.746(7) × 3	
Ba7/Sr8/La9	O12	2.539(5) × 2	3.031
		2.373(5) × 2	
	O13	2.4866(10) × 2	
	O14	2.547(6)	
		2.558(6)	
Co10	O13	1.980(5) × 3	3.090
	O14	1.914(6) × 3	
Co11	O12	1.834(4) × 2	2.792
	O13	1.939(5)	
	O15	1.749(6)	

the 11- and 12-fold coordinated Ba–O polyhedra and the 8-fold coordinated R/Sr–O or R/Ba/Sr–O polyhedra are not drawn. The unit-cell outline is also illustrated. There are two Co_4O_{15} clusters per unit cell that are in turn joined by various lanthanide and alkaline-earth cations that are in 6-fold (octahedral SrO_6), 8-fold (bisdisphenoid $(R/Sr)O_8$), 10-fold (capped trigonal prism, BaO_{10}), and 12-fold (cubic close packed, BaO_{12}) coordination to various oxygen ions. In $Ba_5SrGd_2Co_4O_{15}$, the octahedral cation positions are randomly occupied by an equal amount of Sr and Ba, and the bisdisphenoid cation positions are randomly occupied by 2/3R, 1/6Ba, and 1/6Sr. In $Ba_4Sr_2R_2Co_4O_{15}$, the bisdisphenoid cation positions are randomly occupied by 2/3R and 1/3Sr. Figure 5 gives the coordination environment of Ba exhibiting both 10-fold and 12-fold coordination.

Tables IV(a) and IV(b) give the bond distances of Ba/Sr–O, R–O, and Co–O, and bond valence sum values (V_b) for $Ba_4Sr_2R_2Co_4O_{15}$ and $Ba_5SrR_2Co_4O_{15}$, respectively. The

TABLE V. X-ray powder pattern for $Ba_4Sr_2Gd_2Co_4O_{15}$ ($P6_3mc$ (No. 186), $a = 11.5872(4)$ Å, $c = 6.8169(2)$ Å, $V = 792.63(6)$ Å^3, Z = 2, and $D_x = 6.35$ g cm^{-3}). The symbols "M" and " + " refer to peaks containing contributions from two and more than two reflections, respectively. The symbol * indicates that the particular peak has the strongest intensity of the entire pattern and is designated a value of "999."

d	*I*	*h*	*k*	*l*	*D*	*I*	*h*	*k*	*l*	*d*	*I*	*h*	*k*	*L*
10.035	56	1	0	0	5.0175	6	2	0	0	4.0408	94	2	0	1
3.7928	6	2	1	0	3.4084	38	0	0	2	3.3449	5	3	0	0
3.3143	149	2	1	1	3.2274	75	1	0	2	3.0029	106	3	0	1
2.9378	329	1	1	2	2.8968	999*	2	2	0	2.8194	461	2	0	2
2.5767	35	3	1	1	2.5352	144	2	1	2	2.3874	348	3	0	2
2.3543	134	4	0	1	2.3021	20	3	2	0	2.2162	89	1	0	3
2.2073	55	2	2	2	2.1811	46	3	2	1	2.1558	26	3	1	2
2.0848	71	4	1	1	2.0699	21	2	0	3	2.0204	183	4	0	2
1.9492	5	2	1	3	1.9312	18	3	3	0	1.9252	95	5	0	1
1.9078	17	3	2	2	1.8796	14	3	0	3	1.8423	214	4	1	2
1.8270	40	4	2	1	1.8023	26	5	1	0	1.7602	30	3	1	3
1.7424	14	5	1	1	1.7294	81	5	0	2	1.7042	6	0	0	4
1.6841	8	4	0	3	1.6802	64	3	3	2 M	1.6802	64	1	0	4 M
1.6725	161	6	0	0	1.6572	91	4	2	2	1.6497	8	4	3	0
1.6350	64	1	1	4	1.6172	101	3	2	3	1.6137	125	2	0	4
1.6034	56	4	3	1	1.5933	9	5	1	2	1.5768	7	4	1	3
1.5640	68	5	2	1	1.5545	28	2	1	4	1.5185	67	3	0	4
1.5042	14	5	0	3	1.5014	30	6	0	2	1.4931	5	6	1	1
1.4849	55	4	3	2	1.4689	33	2	2	4	1.4560	9	4	2	3
1.4534	88	5	2	2	1.4484	122	4	4	0	1.4335	21	7	0	0 M
1.4335	21	5	3	0 M	1.4097	59	4	0	4	1.3634	11	6	2	1
1.3449	58	4	1	4	1.3330	23	4	4	2	1.3291	13	7	1	0
1.3214	8	5	3	2	1.3157	17	2	0	5	1.3120	12	5	2	3
1.2990	28	5	0	4	1.2883	19	6	2	2	1.2848	12	5	4	0
1.2778	17	3	3	4	1.2693	25	6	1	3	1.2676	49	4	2	4
1.2626	7	5	4	1	1.2431	11	6	3	1	1.2383	41	7	1	2
1.2336	20	8	0	1	1.2124	46	7	0	3 M	1.2124	46	5	3	3 M
1.2066	29	7	2	1	1.1979	18	4	0	5	1.1937	23	6	0	4
1.1867	12	6	2	3	1.1853	61	6	3	2 M	1.1853	61	4	3	4 M
1.1772	11	8	0	2	1.1745	10	8	1	0	1.1731	21	3	2	5
1.1691	44	5	2	4	1.1587	14	5	5	0	1.1574	18	8	1	1 M
1.1574	18	4	1	5 M	1.1536	51	7	2	2	1.1511	9	6	4	0
1.1362	42	0	0	6	1.1350	15	6	4	1	1.1290	12	7	3	0
1.1278	12	5	0	5	1.1184	46	5	4	3	1.1104	13	8	1	2
1.1070	20	4	2	5	1.1037	15	4	4	4	1.1004	20	9	0	1
1.0970	18	5	5	2 M	1.0970	18	5	3	4 M	1.0949	37	8	2	0
1.0906	9	6	4	2	1.0810	6	8	2	1	1.0789	10	7	2	3
1.0779	14	6	2	4	1.0717	8	7	3	2	1.0597	23	9	0	2
1.0577	114	2	2	6	1.0509	11	4	3	5	1.0481	15	7	1	4
1.0424	34	8	2	2	1.0396	25	6	5	1 M	1.0396	25	5	2	5 M
1.0286	15	7	4	1	1.0154	19	6	3	4	1.0052	33	6	5	2 M
1.0052	33	9	1	2 M	0.9952	78	7	4	2 M	0.9952	78	7	2	4 M
0.9888	8	9	2	0	0.9879	9	7	0	5	0.9864	6	8	2	3
0.9739	18	6	2	5	0.9671	8	8	1	4	0.9656	16	6	6	0
0.9611	21	7	5	0 M	0.9611	21	5	1	6 M	0.9582	7	5	5	4
0.9560	6	2	0	7	0.9539	9	6	4	4	0.9525	6	10	1	0
0.9482	9	8	4	0	0.9432	16	2	1	7	0.9412	11	7	3	4
0.9398	61	6	0	6	0.9392	12	8	4	1	0.9350	15	5	4	5 M
0.9350	15	3	0	7 M	0.9330	16	9	0	4	0.9297	8	8	3	3
0.9290	14	6	6	2	0.9277	23	9	3	0	0.9270	6	6	3	5
0.9251	20	7	5	2	0.9231	6	8	0	5	0.9212	45	8	2	4
0.9176	27	10	0	3 M	0.9176	27	10	1	2 M	0.9116	21	7	2	5
0.9066	33	9	2	3	0.9012	16	10	2	0	0.8951	61	6	5	4 +
0.8938	77	4	4	6 M	0.8938	77	10	2	1 M	0.8904	17	7	0	6 +
0.8898	12	4	1	7	0.8881	34	7	4	4	0.8812	26	11	0	2
0.8795	16	6	4	5	0.8761	18	5	0	7	0.8751	13	8	4	3
0.8701	19	11	1	0 M	0.8701	19	9	4	0 M	0.8663	11	4	2	7
0.8636	12	7	1	6	0.8631	13	9	4	1 M	0.8631	13	9	0	5 M
0.8568	7	5	1	7	0.8552	29	8	5	2					

results of bond valence calculations show that Co atoms in both octahedral and tetrahedral sites are all of a 3+ valence instead of a 2+ valence. From $R = La$ to $R = Gd$, all Co^{3+} sites experience tensile stress, or underbonding (in an over-sized cage environment) as V_b values are all smaller than the ideal valence of 3+. However, the V_b values for the octahedral Co site in the Dy-analog are substantially greater than 3.0 (compressive strain). The V_b values for $Ba_4Sr_2R_2Co_4O_{15}$

and $Ba_5SrR_2Co_4O_{15}$ suggest that all Ba^{2+} and Sr^{2+} sites (except for Ba3) are under tensile stress. The V_b of Ba3 changes from 1.886 to 3.642 in $Ba_4Sr_2R_2Co_4O_{15}$ and from 1.883 to 3.031 in $Ba_5SrR_2Co_4O_{15}$ as the ionic radius decreases from La^{3+} to Dy^{3+} and from La^{3+} to Gd^{3+}, respectively, the Ba3 cage changes from under tensile stress to compressive stress. In the $R = $ Dy analog, the large compressive stress at Ba3 ($V_b = 3.6$) and at Co6 ($V_b = 3.3$) imply maximum strain or the last member (with the smallest lanthanide ion) that $Ba_4Sr_2R_2Co_4O_{15}$ can form. Note that most of the V_b values for R–O in $Ba_4Sr_2R_2Co_4O_{15}$ and $Ba_5SrR_2Co_4O_{15}$ are significantly greater than the ideal value for that site. Since all R sites are mixed with Sr or with Sr and Ba, the ideal V_b value is 2.666 ($2/3 \times 3 + 1/3 \times 2 = 2.666$), the values here, ranging from 2.842 to 3.144 are all greater than 2.666, representing a large compressive stress or overbonding for the R sites except for the phase with $R = $ Dy. All V_b values for the cobalt sites are mostly less than 3.0, suggesting compressive stress.

B. Reference X-ray diffraction patterns

An example of the reference patterns of $Ba_4Sr_2Gd_2Co_4O_{15}$ is given in Table V. In this pattern, the symbols "M" and "+" refer to peaks containing contributions from two and more than two reflections, respectively. The symbol * indicates that the particular peak has the strongest intensity of the entire pattern and has been designated a value of "999." The intensity values reported are integrated intensities rather than peak heights. All patterns have been submitted for inclusion in the Powder Diffraction File (PDF) (ICDD).

IV. SUMMARY

Crystal structure, reference patterns, and TE properties of $Ba_4Sr_2R_2Co_4O_{15}$ ($R = $ La, Nd, Sm, Eu, Gd, and Dy), and $Ba_4Sr_2R_2Co_4O_{15}$ ($R = $ La, Nd, Sm, Eu, and Gd) series of compounds have been determined. The small size of Sr (as compared to Ba) apparently gives rise to the stability of $Ba_4Sr_2Dy_2Co_4O_{15}$, whereas the corresponding $Ba_5SrDy_2Co_4O_{15}$ phase is not stable. Bond valence sum calculations indicated that all Co's adopt 3+ valence states in these compounds. In the $Ba_4Sr_2Dy_2Co_4O_{15}$ analog the large compressive stress at Ba3 ($V_b = 3.6$) and at Co6 ($V_b = 3.3$) imply maximum strain or the last member (with the smallest lanthanide ion) that $Ba_4Sr_2R_2Co_4O_{15}$ can form.

Abe, K., Doi, Y., Hinatsu, Y., and Ohoyama, K. (**2006**). "Magnetic properties of the spin tetramer compound $Ba_6Nd_2Fe_4O_{15}$," Chem. Mater. **18**, 785–789.

Brese, N. E. and O'Keeffe, M. (**1991**). "Bond-valence parameters for solids," Acta Crystallogr. B **47**, 192–197.

Brown, I. D., and Altermatt, D. (**1985**). "Bond-valence parameters obtained from a systematic analysis of the inorganic crystal structure database," Acta Crystallogr. B **41**, 244–247.

Grebille, D., Lambert, S., Bouree, F., and Petricek, V. (**2004**). "Contribution of powder diffraction for structure refinements of aperiodic misfit cobalt oxides," J. Appl. Crystallogr. **37**, 823–831.

Hu, Y. F., Si, W. D., Sutter, E., and Li, Q. (**2005**). "*In situ* growth of *c*-axis-oriented $Ca_3Co_4O_9$ thin films on Si(100)," Appl. Phys. Lett. **86**, 082103.

Larson, A. C. and von Dreele, R. B. (**2004**). *General Structure Analysis System (GSAS)*, Los Alamos National Laboratory Report LAUR 86–748, Los Alamos, USA.

Masset, A. C., Michel, C., Maignan, A., Hervieu, M., Toulemonde, O., Studer, F., and Raveau, B. (**2000**). "Misfit-layered cobaltite with an anisotropic giant magnetoresistance: $Ca_3Co_4O_9$," Phys. Rev. B **62**, 166–175.

Mevs, H. and Müller-Buschbaum, H. (**1990a**). "Zur Kenntnis von $Ba_6La_2Co_4O_{15}$", Z. Anorg. Allg. Chem. **584**, 114–118; ICSD collection code 69635.

Mevs, H. and Müller-Buschbaum, H. (**1990b**). "Neue Verbindungen mit $Ba_6Ln_2M_4^{3+}O_{15}$-Typ: $Ba_6Nd_2Fe_4O_{15}$, $Ba_5SrLa_2Fe_4O_{15}$ und $Ba_5SrNd_2Fe_4O_{15}$," J. Less-Common Metals **158**, 147–152.

Mevs, H. and Müller-Buschbaum, H. (**1990c**). "$Ba_6Nd_2Fe_4O_{15}$: Ein oxometallat mit neuem strukturtyp," J. Less-Common Metals **157**, 173–178.

Mikami, M. and Funahashi, R. (**2005**). "The effect of element substitution on high-temperature thermoelectric properties of $Ca_3Co_2O_6$ compounds", J. Solid State Chem. **178**, 1670–1674.

Mikami, M., Funashashi, R., Yoshimura, M., Mori, Y., and Sasaki, T. (**2003**). "High-temperature thermoelectric properties of single-crystal $Ca_3Co_2O_6$," J. Appl. Phys. **94**, 6579–6582.

Minami, H., Itaka, K., Kawaji, H., Wang, Q. J., Koinuma, H., and Lippmaa, M. (**2002**). "Rapid synthesis and characterization of $(Ca_{1-x}Ba_x)_3Co_4O_9$ thin films using combinatorial methods," Appl. Surface Sci. **197**, 442–447.

Müller-Buschbaum, H. and Martin, F. D. (**1992**). "Syntheses und kristallstruktur von $Ba_{4.5}Ca_{1.5}La_2Fe_4O_{15}$, $Ba_5CaEu_2Fe_4O_{15}$, and $Ba_5CaNd_2Co_4O_{15}$", Z. Anorg. Allg. Chem. **617**, 84–88; ICSD collection code 72338.

Müller-Buschbaum, H. and Uensal, H. (**1996**). "Zur Kenntnis $Ba_6Pr_2Co_4O_{15}$ und $Ba_5SrPr_2Co_4O_{15}$", Z. Naturf., Teil B: Anorg. Chem., Org. Chem. **51**, 453–455; ICSD collection codes 380091 and 380092.

Nolas, G. S., Sharp, J., and Goldsmid, H. J. (**2001**). *Thermoelectric: Basic Principles and New Materials Developments* (Springer, New York).

Rietveld, H. M. (**1969**). "A profile refinement method for nuclear and magnetic structures," J. Appl. Cryst. **2**, 65–71.

Rüter, I. and Müller-Buschbaum, H. k. (**1990**). "Zur Krsitallchemie von oxometallaten der Zusammensetzung $Ba_6Nd_2Al_4O_{15}$ Neue Ergebnisse an $Ba_{4.5}Ca_{1.5}Nd_2Fe_4O_{15}$ und $Ba_5CaSm_2Fe_4O_{15}$," J. Less-Common Metals **162**, 175–180.

Shannon, R. D. (**1976**). "Revised effective ionic radii and systematic studies of interatomie distances in halides and chalcogenides," Acta Crystallogr. A **32**, 751–767.

Terasaki, I., Sasago, Y., and Uchinokura, K. (**1997**). "Large thermoelectric power in $NaCo_2O_4$ single crystals", Phys. Rev. B **56**, 12685–12687.